This article has been accepted for publication in a future issue of this journal, but has not been fully edited. Content may change prior to final publication. Citation information: DOI 10.1109/LRA.2017.2768124, IEEE Robotics and Automation Letters

Subject-specific Assist-as-needed Controllers for a Hand Exoskeleton for Rehabilitation

Priyanshu Agarwal[1] and Ashish D. Deshpande[2]

***Abstract*—Robotic rehabilitation of the hands from a neuromuscular impairment such as stroke requires controllers that could provide subject-specific assistance and result in fastest possible recovery. We present two such assist-as-needed controllers for a hand exoskeleton called Maestro that is designed to provide accurate torque assistance to a subject. Learned force-field control is a novel control technique in which a neural-network-based model of the required torques is learned off-line for a specific subject and then used to render a force-field to assist the finger motion to follow a target trajectory. Adaptive assist-as-needed control, on the other hand, estimates the coupled finger-exoskeleton system torque requirement of a subject using a radial basis function (RBF) network and adapts the RBF magnitudes in real-time to provide a feedforward assistance for accurate trajectory tracking. Experiments with a healthy subject on Maestro showed that while the force-field control is non-adaptive and there is less control on the speed of execution of the task, it is safer as it does not apply increased torques if the finger motion is restricted. On the other hand, adaptive assist-as-needed controller adapts to the changing needs of the coupled finger-exoskeleton system and helps in performing the task with a consistent speed, however, applies increased torques in case of restricted motion and is therefore, potentially less safe.**

***Index Terms*—Rehabilitation Robotics, Prosthetics and Exoskeletons, Wearable Robots**

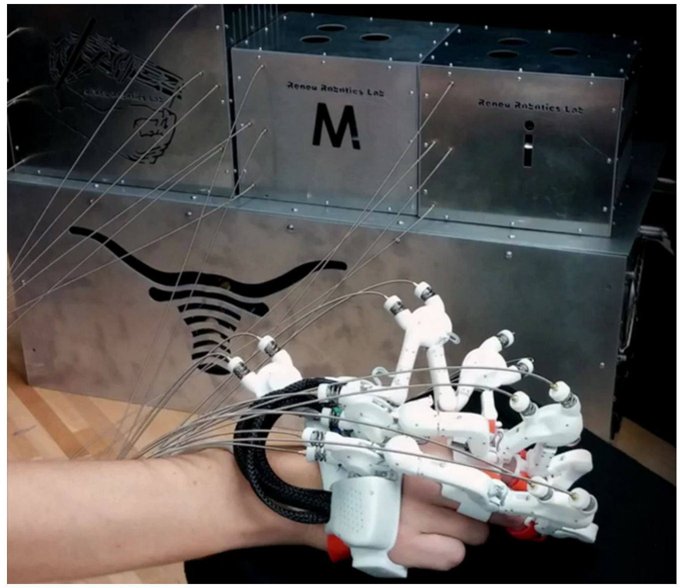

Fig. 1. Hand exoskeleton system used for carrying out experiments with the two developed controllers.

I. INTRODUCTION

REHABILITATION of hands using robotic devices has gained momentum in the last decade as these devices can be used to assess recovery progress and provide repetitive and intensive training with significantly less manual labor [1], [2], [3], [4], [5]. Evidence in the rehabilitation literature suggests that in general force-control based strategies can be more effective than position-based control alone [6]. While several force-based advanced controllers have been developed for rehabilitation of both the upper and lower limbs, the controllers used for hand rehabilitation have primarily been limited to position control [7], [8]. This is mainly because force control of hand exoskeletons is challenging with many degrees of freedom of the hand in a limited space. Furthermore, an understanding of what control algorithms could best leverage neural plasticity and achieve best possible functional recovery using these devices is currently missing.

Different hand impairments have distinct therapy requirements based on the nature, severity or acuteness of the impairment and state of recovery. For example, during acute phase of stroke when the hand digits do not have full range of motion, the requirement is to provide appropriate assistance for passively moving the digits through their range of motion without focusing on the positional accuracy of the digits. Later, when the full passive range of motion of the hand digits is recovered, the requirement is to encourage the subject to exert forces with the digits and actively participate in the training tasks. Finally, when the subject could actively generate grasping forces the requirement changes to further train the subject to achieve accurate finger positioning for fine manipulation tasks. This constantly changing training requirement demands controllers that could accommodate and adapt to the changing requirements of a specific subject.

Torque requirement for impaired subjects vary drastically based on the degree and type of impairement, which makes the use of basic force control inadequate without an estimate of the subject-specific torque requirement. Such a control also fails to

Manuscript received: May, 23, 2017; Revised September, 8, 2017; Accepted October, 3, 2017.

This paper was recommended for publication by Editor Allison M. Okamura upon evaluation of the Associate Editor and Reviewers' comments. This work was supported, in part, by the National Science Foundation (NSF) grant CNS-1135949, National Aeronautics and Space Administration (NASA) grant NNX12AM03G and Graduate School Continuing Fellowship offered by The University of Texas at Austin.

[1]Priyanshu Agarwal is with the Mechanical Engineering Department, Rice University, 6100 Main St., Houston TX 77005, USA. This work was done when he was a PhD student at University of Texas at Austin. priyanshu.agarwal@rice.edu

[2]Ashish D. Deshpande is with Faculty of Mechanical Engineering, University of Texas at Austin, Austin, Texas 78712, USA ashish@austin.utexas.edu

Digital Object Identifier (DOI): see top of this page.

achieve desired movement due to lack of error correction in the joint position. Impedance control [9] and admittance control [10], [11], which are capable of compliantly interacting with the human limb, have been adopted to improve the accuracy of position tracking [12], [13]. However, impedance control requires high stiffness to create accurate movement. This is particularly true for the finger joints where stiffness varies significantly within the range of motion [14], especially in the absence of accurate subject-specific stiffness model of the finger joints. Furthermore, certain impairments (e.g. spastic catch phenomena and changing nature of spasms in spastic finger muscles [16] and inflammatory joint disease such as rheumatoid arthritis [17]) could lead to accidental locking of the finger joints. A high exoskeleton impedance could lead to a scenario where large torques are applied at the finger joints due to their sudden stalling [15], which would be uncomfortable and unsafe for the subject. Also, the users tend to slack and mostly rely on the assistive force provided by impedance control, which reduces patient involvement in the task and inhibits learning [18]. Thus, there is a need to learn subject-specific models of the required assistance along with a means to adapt the model-based assistance for hand rehabilitation.

We have developed a hand exoskeleton system, called Maestro, that allows for control of the torques applied at the various digits of the hand [19], [20]. The exoskeleton consists of three modules to actively assist the index and middle fingers and the thumb. Each finger module has two actuated degrees of freedom (DOF) to assist the motion at the metacarpophalangeal (MCP) and proximal interphalangeal (PIP) joints of the finger. Miniature Bowden-cable-based series elastic actuators allow to achieve bidirectional torque control of the actuated exoskeleton joints [29]. These actuators also make the device highly backdrivabile while keeping the reflected inertia low. In this work, we develop two assist-as-needed controllers for Maestro. Learned force-field control learns a subject-specific model of the required joint torques using a neural network and use this model to build a force-field to assist the finger joint motion of the subject. Adaptive assist-as-needed control, on the other hand, varies the amount of assistance based on online estimation of the subject performance using measurements, to encourage active participation.

A force-field control has been developed for a lower limb exoskeleton, which provided only a constant assistance along the task trajectory [21], [22], was not subject-specific and did not have any learning aspect. Such a controller is not appropriate for a hand exoskeleton. This is because for hand digits the joint stiffness changes considerably within the range of motion, so accurate force-field assistance for the specific subject is needed along the task trajectory to achieve the task at desired velocities. Also, the previous force-field control did not take into account the fact that the nature of assistance can vary in the workspace due to the non-homogeneous residual motor capabilities of a subject [23]. A few upper and lower limb exoskeletons have also implemented adaptive assist-as-needed control [24], [25], [26].

There are several differences in our implementation and the existing implementations of these controllers. First, the controllers presented in the past were all implemented in the task space i.e. the assistance is modulated to meet the tracking requirement of only the end-effector of the device [24], [25], [21], [22]. Our controllers, on the other hand, are implemented in the joint space i.e. the assistance is modulated to meet the tracking requirement of each joint individually. Previous work suggests that better motor learning takes place when haptic training of complex movements is conducted by anatomically decomposing the complex motion [27]. Our implementation readily allows for this type of training by choosing appropriate desired joint angle trajectory for each joint individually. Second, our joint-space-based approach provides a mapping of the torque requirement at individual human joint, which can be used to diagnose the nature of impairment and prescribe future course of therapy based on this understanding of recovery. Finally, the learning of the required assistance takes place in the joint angle space in our implementation of adaptive assist-as-needed control as opposed to the task position and velocity space. In addition, such assist-as-needed controllers have never been implemented for a hand exoskeleton in the past. Furthermore, the term adaptive assist-as-needed control have been used in the past to represent both the types of control, however, these controllers have never been compared in the past.

We implement the learned force-field and adaptive assist-as-needed controllers on Maestro and conduct experiments with a healthy subject to validate their performance. Specifically, we make the following contributions: (i) a novel neural-network-based learned force-field control that allows to capture the non-linear nature of required assistance, (ii) learned force-field and adaptive assist-as-needed controllers for Maestro, (iii) compare and contrast the two assist-as-needed controllers using experimental results, and (iv) present three-dimensional torque mapping for the finger joints, which could be used to classify and diagnose hand impairments. The controllers presented in this work are general and can be implemented on each digit of the exoskeleton. Multiple digits of the device can be actuated by defining appropriate desired trajectories for each digit. Since the index finger exoskeleton acts as the basis of the design for each digit, in this work we conduct experiments with the index finger module to validate these controllers. Portions of this work have previously been presented in [15], [28].

II. CONTROLS

In this section, we present two assist-as-needed controllers that learn subject-specific models of the coupled hand exoskeleton system to provide appropriate torques as per the needs of the subject.

A. Learned Force-field Control

Learned force-field is designed to assist subjects in achieving a coordinated flexion-extension motion at the MCP and PIP finger joints. In general, a force-field control renders a tunnel-like force-field in the configuration space, which guides the motion of the limb to evolve along the specified target path [30], [22]. The key feature of this type of control is that the target path and the control input is only a function of the

This article has been accepted for publication in a future issue of this journal, but has not been fully edited. Content may change prior to final publication. Citation information: DOI 10.1109/LRA.2017.2768124, IEEE Robotics and Automation Letters

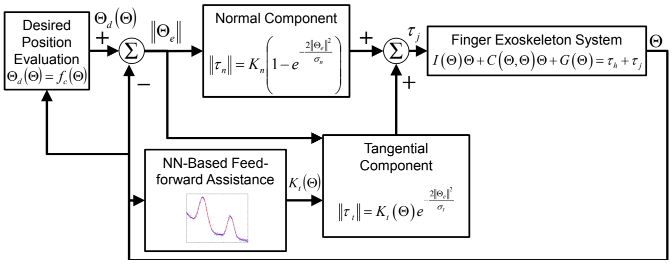

Fig. 2. Overview of the learned force-field control implemented on the finger module of Maestro.

current system configuration and not of time explicitly. To learn the torque mapping as a function of the exoskeleton joint angles we use a neural network model. This trained network is then used to render a force-field that provides the assistance necessary to achieve the coordinated motion at the finger joints (Fig. 2). This controller, therefore, learns the needs of a specific subject and provide appropriate assistance to the subject.

1) Subject-specific Data: We first control the exoskeleton in impedance control mode to obtain the subject-specific nonlinear exoskeleton joint torques to joint angles mapping (Fig. 3) [15]. We chose sinusoidal joint angle trajectories, which have been shown to represent the finger joint motion while performing different tasks [31], as the desired motion at the finger joints, by gradually increasing controller impedance. For this motion, the torque vary in a closed contour at both the exoskeleton joints (Fig. 3(c)) due to the viscous and frictional dissipation at the finger joints [32], which results in hysteresis loops. The desired sinusoidal joint angle trajectories manifest as a linear target trajectory in the exoskeleton configuration space (Fig. 3(d)).

2) Learning System Dynamics: We use a neural network with one hidden layer and three perceptrons to learn the torque to joint angle mapping at the two exoskeleton joints. Different networks are learned for flexion and extension torque-angle mapping, since the mapping showed a hysteresis loop. We use linear transfer functions for the input and output layers. Some studies have shown that networks with hyperbolic tangent sigmoid as a transfer function are more generalizable [33] and perform better than networks with other types of transfer functions [34], [35]. Therefore, we use hyperbolic tangent sigmoid transfer function for the perceptrons in the hidden layer.

3) Force-field Control: The force-field in our implementation is learned in the joint space of the finger module. The torque vector (τ) in learned force-field control has a normal ($\mathbf{\tau_n}$) and a tangential ($\mathbf{\tau_t}$) torque component, which act at the exoskeleton MCP and PIP joints (Eq. (1)). The tangential component assists in moving along the target trajectory and the normal component pushes the finger towards the target trajectory. It is the assistance along the target trajectory that varies significantly from subject to subject based on the type and degree of impairment. So, we learn the gain for the tangential component of the force field ($\mathbf{K_t}(\mathbf{\Theta})$) using the neural network model to guide the finger motion along the target path in the exoskeleton joint angle space.

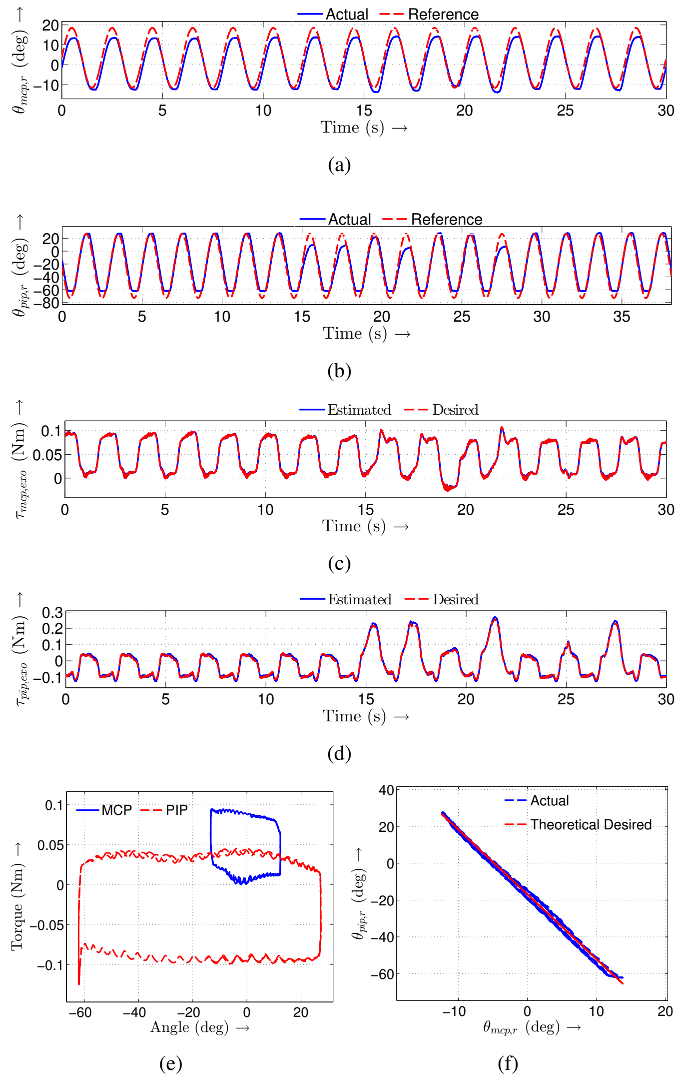

Fig. 3. Results from the impedance control of the index finger module with sinusoidal desired trajectories at the exoskeleton MCP and PIP joints. (a) Exoskeleton MCP joint relative angle tracking, (b) exoskeleton PIP joint relative angle tracking, (c) exoskeleton joint torque with respect to the respective relative joint angle, (d) exoskeleton relative PIP joint angle with respect to relative MCP joint angle, (e) exoskeleton joint torque variation with respect to the respective exoskeleton joint angle at the MCP and PIP joints and (f) exoskeleton MCP joint angle variation with respect to the exoskeleton PIP joint angle.

$$\tau = \mathbf{\tau_n} + \mathbf{\tau_t} \tag{1}$$

$$\begin{aligned} \|\mathbf{\tau_n}\| &= \mathbf{K_n}\left(1 - e^{-\frac{2\|\mathbf{\Theta_e}\|^2}{\sigma_n}}\right) \\ \|\mathbf{\tau_t}\| &= \mathbf{K_t}(\mathbf{\Theta})e^{-\frac{2\|\mathbf{\Theta_e}\|^2}{\sigma_t}} \end{aligned} \tag{2}$$

where $\mathbf{K_n}$ and $\mathbf{K_t}(\mathbf{\Theta})$ are the gain vectors for the normal and tangential force field assistance, respectively. $\mathbf{\Theta}$ is the current angular joint position vector of the exoskeleton joints. $\|\mathbf{\Theta_e}\|$ is the distance between the current exoskeleton joints

This article has been accepted for publication in a future issue of this journal, but has not been fully edited. Content may change prior to final publication. Citation information: DOI 10.1109/LRA.2017.2768124, IEEE Robotics and Automation Letters

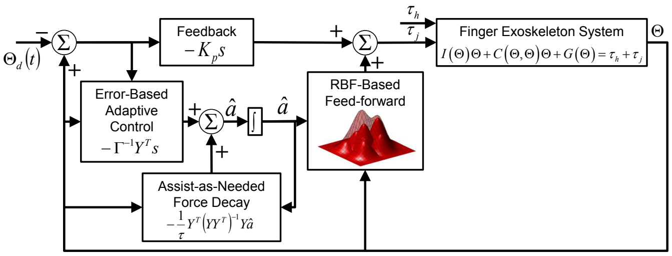

Fig. 4. Overview of the adaptive-assistance-based control implemented on the finger module of Maestro.

position and the closest configuration on the target trajectory. Two force field tunnels with diameters σ_n and σ_t created in the joint angle space around the target path are given by Eq. (2). The magnitude of the normal component increases to $\mathbf{K_n}$ outside of the tunnel and gradually reduces to zero as one approaches the target path inside the tunnel. The magnitude of the tangential component, on the other hand, is close to zero outside the tunnel and gradually increases to $\mathbf{K_t}(\mathbf{\Theta})$ as one approaches the target path inside the tunnel. An analytical expression is obtained for $\mathbf{\Theta_e}$ by projecting the current exoskeleton joint angle state on the target line segment contour ($\mathcal{C}$) (Eq. (3)).

$$\|\mathbf{\Theta_e}\| = \min_{\mathbf{\Theta_d} \in \mathcal{C}} \|\mathbf{\Theta} - \mathbf{\Theta_d}\| \tag{3}$$

Since different networks are learned for flexion and extension motion, the tangential gain is determined by switching between the two networks based on whether the upper ($\mathbf{\Theta}_{ub}$) or lower ($\mathbf{\Theta}_{lb}$) exoskeleton joint angle limit is crossed (Eq. (4)).

$$\mathbf{K_t}(\mathbf{\Theta}) = \begin{cases} \mathbf{K_{tf}}(\mathbf{\Theta}), & \text{if } \mathbf{\Theta} \le \mathbf{\Theta}_{lb} \\ \mathbf{K_{te}}(\mathbf{\Theta}), & \text{if } \mathbf{\Theta} \ge \mathbf{\Theta}_{ub} \end{cases} \tag{4}$$

where $\mathbf{K_{tf}}(\mathbf{\Theta})$ and $\mathbf{K_{te}}(\mathbf{\Theta})$ are the gain vectors for the tangential component of the force field assistance for the flexion and extension motion, respectively, as learned using neural network.

In learned force-field control, the neural network mapping is static and therefore, the torque requirement is not updated with either change in the frequency of motion or inherent changes in the required finger torque due to changes in the neuromuscular characteristics of the finger. This is a major limitation of this type of control. So, next we implement an adaptive assist-as-needed controller to address this limitation.

B. Adaptive-assistance-based Control

Adaptive assist-as-needed control learns a dynamics model of the coupled finger-exoskeleton system and the ability and effort of a specific subject in real-time [24] (Fig. 4).

1) Adaptive Controller for Learning Coupled System Dynamics: The coupled dynamics of the finger exoskeleton system can be expressed as in Eq. (5).

$$\mathbf{I}(\mathbf{\Theta})\ddot{\mathbf{\Theta}} + \mathbf{C}(\mathbf{\Theta}, \dot{\mathbf{\Theta}})\dot{\mathbf{\Theta}} + \mathbf{G}(\mathbf{\Theta}) = \tau_{\mathbf{j}} + \tau_{\mathbf{h}} \tag{5}$$

where $\mathbf{\Theta}$ is the 2×1 vector of exoskeleton MCP and PIP joint angular position, $\boldsymbol{I}(\mathbf{\Theta})$ is the inertia matrix, $\boldsymbol{C}(\mathbf{\Theta}, \dot{\mathbf{\Theta}})$ is the matrix representing Coriolis and centrifugal terms, $\mathbf{G}$ is the vector representing gravitational terms, $\tau_{\mathbf{j}}$ is the 2×1 vector representing the torques applied by the actuated exoskeleton MCP and PIP joints and $\tau_{\mathbf{h}}$ is the 2×1 vector representing the torques applied by the human subject at the exoskeleton MCP and PIP joints.

We define a sliding surface ($\mathbf{s}$) to formulate the joint angle tracking problem (Eq. (6)).

$$\mathbf{s} = \dot{\tilde{\mathbf{\Theta}}} + \Lambda\tilde{\mathbf{\Theta}} = (\dot{\mathbf{\Theta}} - \dot{\mathbf{\Theta}}_d) + \Lambda(\mathbf{\Theta} - \mathbf{\Theta}_d) \tag{6}$$

where $\tilde{\mathbf{\Theta}} = \mathbf{\Theta}(t) - \mathbf{\Theta_d}(t)$ is the tracking error with $\mathbf{\Theta_d}(t)$ as the desired joint angle trajectory. Λ is a 2×2 constant, positive definite and symmetric matrix.

For the finger-exoskeleton system the contribution of inertial effects is small. Therefore, in our formulation we only consider the position-dependent terms in the system dynamics (Eq. (5)) and define a position-dependent regressor matrix. Since the system parameters appear linearly in Eq. (5), the estimated system dynamics can be expressed as a product of the unknown system parameters ($\hat{\mathbf{a}}$) and the regressor matrix ($\mathbf{Y}(\mathbf{\Theta})$) (Eq. (7)). The torque control law for the system is then given by Eq. (8)

$$\hat{\mathbf{G}}(\mathbf{\Theta}) - \hat{\tau}_{\mathbf{h}} = \mathbf{Y}(\mathbf{\Theta})\hat{\mathbf{a}} \tag{7}$$

$$\tau_{\mathbf{j}} = \mathbf{Y}(\mathbf{\Theta})\hat{\mathbf{a}} - \mathbf{K_p}s \tag{8}$$

where $\mathbf{K_p}$ is a symmetric positive definite feedback gain matrix.

We approximate the arbitrary torque surface with respect to the exoskeleton joint angles using a radial basis function (RBF) (Eq. (9)) network.

$$\phi_n = e^{-\dfrac{\|\mathbf{\Theta} - \mu_{\mathbf{n}}\|^2}{2\sigma^2}} \tag{9}$$

We use a 25 RBF network to approximate the torque-angle relationship throughout the workspace by partitioning the rotational DOF into five equally spaced intervals at both the MCP and PIP joints of the exoskeleton. The regressor matrix is then given by Eq. (10).

$$\mathbf{Y}^{2\times50} = \begin{bmatrix} \mathbf{\Phi}^T & \mathbf{0} \\ \mathbf{0} & \mathbf{\Phi}^T \end{bmatrix} \tag{10}$$

where $\mathbf{\Phi} = [\phi_1 \ \phi_2 \ \ldots \phi_{25}]$. The regressor matrix takes into account both the joint angles to determine the torque at each joint. The parameter update law is given by Eq. (11) and it can be shown using Lyapunov stability analysis that the controller is uniformly ultimately bounded [25].

$$\dot{\hat{\mathbf{a}}} = -\mathbf{\Gamma}^{-1}\mathbf{Y}^T\mathbf{s} \tag{11}$$

2) Assist-as-needed Controller Modification: Experiments have shown that subjects slack when full assistance is provided through the controller, which inhibits motor recovery [24]. To account for this effect, the parameter update law is modified (Eqs. (12) and (13)) to decay the applied torques when errors are small as proposed in [24].

$$\frac{\partial}{\partial t}(\mathbf{Y}\hat{\mathbf{a}}) = \mathbf{Y}\dot{\hat{\mathbf{a}}} = -\frac{1}{\tau}\mathbf{Y}\hat{\mathbf{a}} \tag{12}$$

$$\dot{\hat{\mathbf{a}}} = -\Gamma^{-1}\mathbf{Y}^T\mathbf{s} - \frac{1}{\tau}\mathbf{Y}^T\left(\mathbf{Y}\mathbf{Y}^T\right)^{-1}\mathbf{Y}\hat{\mathbf{a}} \tag{13}$$

This article has been accepted for publication in a future issue of this journal, but has not been fully edited. Content may change prior to final publication. Citation information: DOI 10.1109/LRA.2017.2768124, IEEE Robotics and Automation Letters

where τ is the time constant for the parameter decay.

III. Experiments

Experiments were conducted with the finger module to validate and understand the advantages and disadvantages of the developed controllers. A healthy subject (male, age 29 years) participated in the study, after their written consent is obtained. The study is approved by the institutional review board at The University of Texas at Austin. We also assess the stability of the controller and safety of the device by occasionally impeding the motion of the finger, while conducting these experiments.

A. Learned Force-field Control

We first learned the subject's torque-angle relationship during the flexion and extension motion at the index finger joints using two neural networks. These trained subject-specific networks are then used to render a force-field with a desired trajectory in the joint angle space. To get an accurate estimate of the passive requirement of the finger joints using impedance control, the subject is asked to relax the finger muscles while the torque data is collected. During the controller test phase, the subject is asked to follow the desired motion, while the controller assisted the subject using the learned force-field.

B. Adaptive-assistance-based Control

In this experiment, we assessed the adaptability of the controller to a subject's requirement, which results in improved joint angle trajectory tracking performance. We used sinusoidal joint angle trajectories as the desired motion at the two index finger joints.

1) Healthy Subject Experiments: We first conducted two experiments with the unaltered finger module to test if the system could adapt to meet the assistance requirement of the subject. For the first experiment, the subject was asked to keep the finger passive while the controller adapted to the joint torque requirement of the subject. For the second experiment, the subject was asked to impede the exoskeleton motion to assess how quickly the controller could react to the changed torque requirement.

2) Stiffened Exoskeleton Subject Experiments: Stiffening of the finger PIP joint is one of the most common and most serious problem observed in several hand impairments [36], [37], [38]. To validate the effectiveness of the adaption algorithm, we conducted an experiment with an exoskeleton that is stiffened at the PIP joint with elastic rubber bands to simulate increased PIP joint stiffness. The subject was asked to keep the finger passive and the adaptability of the controller to the increased PIP joint stiffness is assessed.

IV. Results

In this section, we present the fitting statistics for the learned neural networks and present results from the aforementioned experiments.

TABLE I
MODEL FITTING STATISTICS (MEAN SQUARED ERROR) FOR THE NEURAL NETWORKS LEARNED TO REPRESENT THE TORQUE-ANGLE RELATIONSHIP FOR THE FLEXION AND EXTENSION MOTIONS.

Motion	Training ($\times 10^{-6}$)	Validation ($\times 10^{-6}$)	Testing ($\times 10^{-6}$)	Overall ($\times 10^{-6}$)
Flexion	3.64	3.87	3.47	3.65
Extension	5.88	8.90	4.38	6.11

A. Learned Force-field Control

The performance of the learned force-field control depends on the accuracy with which the underlying neural network can predict the desired joint torques given the joint angles.

1) Neural Network Fitting Results: The mean squared error for both the trained flexion and extension networks is of the order of 10^{-6} in training, validation and testing (Table I). A comparison of the predicted data with the measured data shows that the learned model is able to predict the exoskeleton joint torques accurately (Fig. 5).

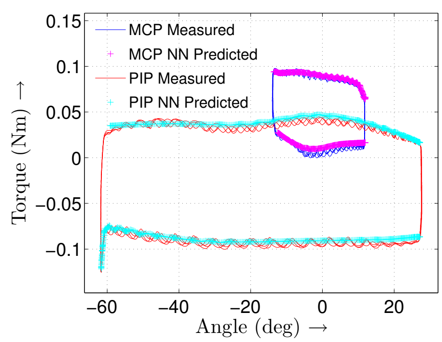

Fig. 5. Comparison of the learned neural-network-based predicted exoskeleton joint torques with those estimated by the series elastic actuator controller in real-time (labeled as measured). (Best viewed in color)

2) Hand Exoskeleton Control: The system is able to achieve coordinated motion at the two exoskeleton joints (Fig. 6(e)). There are several reasons for some deviation that is observed between the actual and desired trajectories. First, the torque assistance that was learned using impedance control was learned with a compliant controller to limit the amount of torque that was applied at the finger joints. Since the finger stiffness changes drastically within its range of motion, the compliant controller is designed to not track the desired trajectory strictly in the high stiffness region of the finger range of motion (Fig. 3(a) and (b)). Second, the torque induced by the subject on the device varies during every repetition of the motion. Third, the constants used to generate the normal component of the force-field are chosen to ensure some compliance in control. Finally, the large deviation in few trials from the theoretically desired trajectory is due to external blocking of the finger motion to assess how the controller reacts to external disturbance, which may be present due to the nature of a finger impairment (Section I).

Force-field control also does not apply excessive torques when the motion is externally blocked at time 22 and 31 seconds (Figs. 6(a),(b) and (c)). However, the velocity with

This article has been accepted for publication in a future issue of this journal, but has not been fully edited. Content may change prior to final publication. Citation information: DOI 10.1109/LRA.2017.2768124, IEEE Robotics and Automation Letters

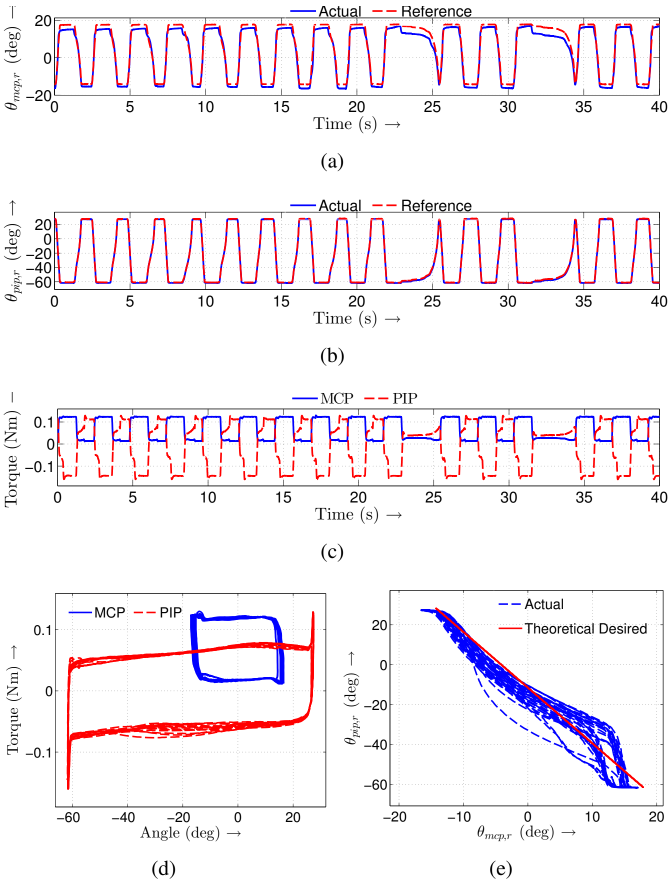

Fig. 6. Results from force-field control of the index finger exoskeleton with a linear relationship between MCP and PIP joint angles as the desired trajectory (a) Exoskeleton MCP joint relative angle tracking, (b) exoskeleton PIP joint relative angle tracking, (c) exoskeleton joint torque with respect to the respective relative joint angle and (d) exoskeleton relative PIP joint angle with respect to relative MCP joint angle.

which the trajectory is traced is not accurately controlled (Figs. 6(a) and (b)). Force-field control allows to achieve coordinated motion at the finger joints and is good for training for the tasks that only need joint angle coordination, while not applying excessive torques in case of an uncertain external disturbance.

B. Adaptive-assistance-based Control

1) Healthy Subject Experiments: In the first experiment, the system is able to adapt to the torque requirement of the subject. The feedforward component of the torque increases gradually, while the feedback component reduces at both the joints (Figs. 7(a) and (b)). The unknown learned parameters also tend to converge to their respective values (Figs. 7(c) and (d)). The root mean square (RMS) tracking error reduced from 5° to 3° at the MCP joint and from 3.5° to under 2° at the PIP joint from the initial to final 10 seconds showing that the adaptive assist-as-needed control improved the tracking performance (Figs. 7(g) and (h)).

In the second experiment, when the finger motion is impeded by the subject, the controller reacted by increasing the applied torque (at time 66 and 86 seconds in Fig. 8). Also, as soon as the externally applied torque is removed the

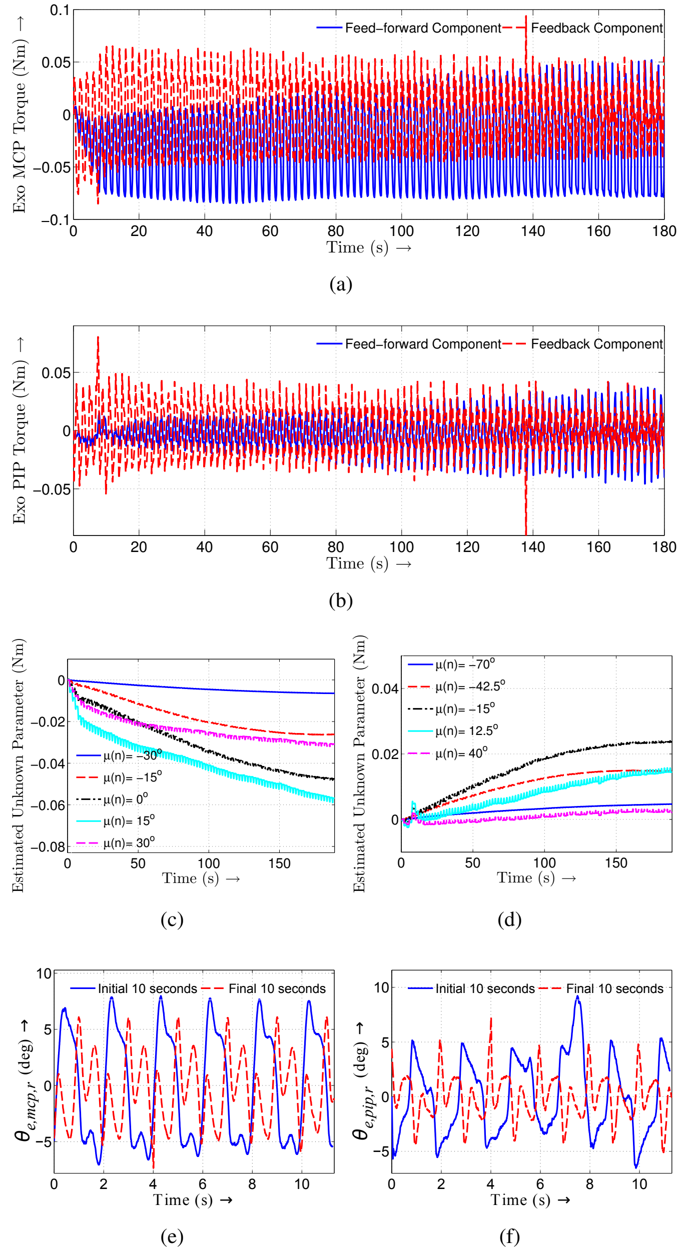

Fig. 7. Results from adaptive assist-as-needed control experiments of the index finger exoskeleton with a healthy subject. (a) Exoskeleton MCP joint feedforward and feedback torque component, (b) exoskeleton PIP joint feedforward and feedback torque component, (c) parameter adaptation results for 5 out of 25 parameters ($\mu_{\mathbf{n}} = [\mu(n) \ -70°]^T$) that contributed to the MCP joint torque (d) parameter adaptation results for 5 out of 25 parameters ($\mu_{\mathbf{n}} = [-30° \ \mu(n)]^T$) that contributed to the PIP joint torque, (e) exoskeleton joint torque variation with respect to the joint angles, (f) exoskeleton MCP angle with respect to the PIP joint angle, (g) MCP joint tracking error for the initial and final 10 seconds and (h) PIP joint tracking error for the initial and final 10 seconds. (Best viewed in color)

controller torque returned to the original value demonstrating that the controller is quite reactive and can quickly adapt to the changing requirements of a subject. However, when the finger motion is accidentally blocked the system applied increased torques at both the finger joints, which might not be safe for the subject.

2) Stiffened Exoskeleton Subject Experiments: Experiments with the stiffened exoskeleton also showed similar results

This article has been accepted for publication in a future issue of this journal, but has not been fully edited. Content may change prior to final publication. Citation information: DOI 10.1109/LRA.2017.2768124, IEEE Robotics and Automation Letters

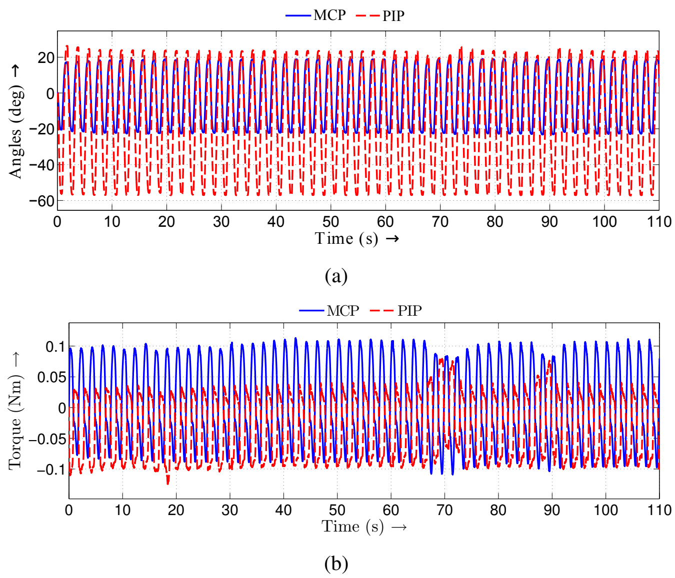

Fig. 8. Adaptive assist-as-needed control experiment with impeded finger motion at time 66 sec and 86 sec. (a) MCP and PIP exoskeleton joint angle with respect to time and (b) MCP and PIP joint torques with respect to time. The joint torque magnitude increases when the finger motion is impeded.

(Figs. 9). RMS tracking error in this case reduced from 5° to under 3° for the MCP joint and from over 4° to 2.5° for the PIP joint (Figs. 9(g) and (h)).

3) Learned Torque Mapping: : A comparison of the three-dimensional learned RBF torque mapping at MCP and PIP joints between the normal and stiffened PIP joint shows that while the torque requirement at the PIP joint has increased considerably the torque mapping at the MCP joint has changed (Fig. 10). This learned torque mapping of the finger joints can also be used to classify hand impairments and further aid the diagnosis of hand impairments.

V. Conclusion

We developed two subject-specific assist-as-needed controllers for a hand exoskeleton, called Maestro. Experiments with the finger exoskeleton showed that the learned force-field control can achieve coordinated motion at the finger joints. Also, the adaptive assist-as-needed control can quickly adapt to the changing requirements of a subject and track the desired joint angle trajectories with small RMS errors (3°and 2 °at MCP and PIP joint, respectively).

Our study suggests that rehabilitation therapy where the goal is to train for time critical tasks and where accurate tracking of the desired joint angle trajectories is needed, adaptive assist-as-needed control would be a better choice. On the other hand, therapy where the coordination between the joints is important rather than the timeliness of the motion, learned force-field control would be more useful. Learned force-field control is in general safer than the adaptive assist-as-needed control, as it does not lead to the application of increased torques if the motion is accidentally stalled. These experiments suggest that a single controller might not be suitable for every neuromuscular impairment. This requires that a repository of subject-specific controllers be developed and the right controller be chosen based on the goals of the therapy and the nature of impairment. In the future, we plan to develop a controls framework in collaboration with therapists that could sense and learn the most suitable control strategy for a specific subject and seamlessly switch strategy based on the therapy goals and subject's needs.

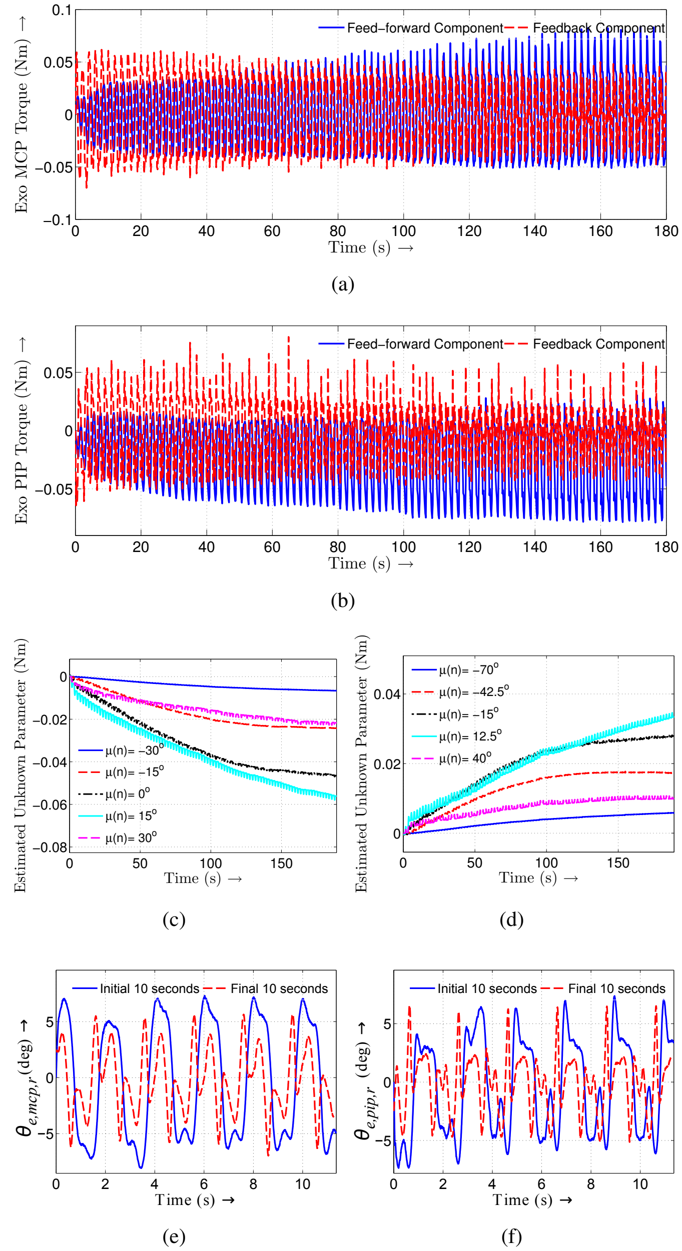

Fig. 9. Results from adaptive assist-as-needed control experiments of the index finger exoskeleton with stiffened exoskeleton PIP joint. (a) Exoskeleton MCP joint feedforward and feedback torque components, (b) exoskeleton PIP joint feedforward and feedback torque components, (c) parameter adaptation results for 5 out of 25 parameters ($\mu_{\mathbf{n}} = [\mu(n) \;\; -70°]^T$) that contributed to the MCP joint torque (d) parameter adaptation results for 5 out of 25 parameters ($\mu_{\mathbf{n}} = [-30° \;\; \mu(n)]^T$) that contributed to PIP joint torque, (e) exoskeleton joint torque variation with respect to the joint angles, (f) exoskeleton MCP angle with respect to the PIP joint angle, (g) MCP joint tracking error for the initial and final 10 seconds and (h) PIP joint tracking error for the initial and final 10 seconds. (Best viewed in color)

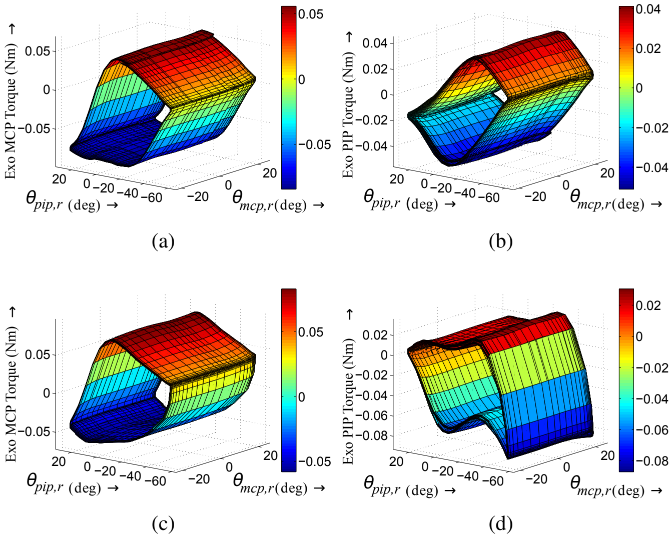

Fig. 10. Three-dimensional torque mapping of the index finger joints learned using adaptive assist-as-needed control. (a) and (b) shows the torque mapping of MCP and PIP joint, respectively, for the healthy subject. (c) and (d) shows the torque mapping of MCP and PIP joint, respectively, with the stiffened exoskeleton PIP joint. The color bar represents the magnitude of the learned torque at a specific configuration. (Best viewed in color)

REFERENCES

[1] L. Dovat, O. Lambercy, B. Salman, V. Johnson, T. Milner, R. Gassert, E. Burdet, and T. C. Leong, "A technique to train finger coordination and independence after stroke," *Disability & Rehabilitation: Assistive Technology*, vol. 5, no. 4, pp. 279–287, 2010.

[2] P. S. Lum, S. B. Godfrey, E. B. Brokaw, R. J. Holley, and D. Nichols, "Robotic approaches for rehabilitation of hand function after stroke," *Amer. Jou. Phy. Med. & Rehab.*, vol. 91, no. 11, pp. S242–S254, 2012.

[3] C. H. Hwang, J. W. Seong, and D.-S. Son, "Individual finger synchronized robot-assisted hand rehabilitation in subacute to chronic stroke: a prospective randomized clinical trial of efficacy," *Clinical Rehabilitation*, vol. 26, no. 8, pp. 696–704, 2012.

[4] E. A. Susanto, R. K. Tong, C. Ockenfeld, and N. S. Ho, "Efficacy of robot-assisted fingers training in chronic stroke survivors: a pilot randomized-controlled trial," *JNER*, vol. 12, no. 1, p. 42, 2015.

[5] P. Agarwal, R. R. Neptune, and A. D. Deshpande, "A simulation framework for virtual prototyping of robotic exoskeletons," *Journal of biomechanical engineering*, vol. 138, no. 6, p. 061004, 2016.

[6] L. Marchal-Crespo and D. J. Reinkensmeyer, "Review of control strategies for robotic movement training after neurologic injury," *Journal of Neuroengg. and Rehab.*, vol. 6, no. 1, p. 20, 2009.

[7] A. Wege and G. Hommel, "Develop. and control of a hand exoskeleton for rehab. of hand injuries," in *IROS*, 2005, pp. 3046–3051.

[8] S. Ueki, H. Kawasaki, S. Ito, Y. Nishimoto, M. Abe, T. Aoki, Y. Ishigure, T. Ojika, and T. Mouri, "Development of a hand-assist robot with multi-degrees-of-freedom for rehabilitation therapy," *IEEE/ASME Transactions on Mechatronics*, vol. 17, no. 1, pp. 136–146, 2012.

[9] N. Hogan, "Impedance control: An approach to manipulation: Part II–Implementation," *JDSMC*, vol. 107, no. 1, pp. 8–16, 1985.

[10] J. K. Salisbury, "Active stiffness control of a manipulator in Cartesian coordinates," in *IEEE Dec. and Contr.*, vol. 19, 1980, pp. 95–100.

[11] M. T. Mason, "Compliance and force control for computer controlled manipulators," *IEEE Tran. SMC*, vol. 11, no. 6, pp. 418–432, 1981.

[12] G. Aguirre-Ollinger, J. E. Colgate, M. A. Peshkin, and A. Goswami, "Active-impedance control of a lower-limb assistive exoskeleton," in *IEEE ICORR*, 2007, pp. 188–195.

[13] R. Colombo, F. Pisano, S. Micera, A. Mazzone, C. Delconte, M. C. Carrozza, P. Dario, and G. Minuco, "Robotic techniques for upper limb evaluation and rehabilitation of stroke patients," *IEEE TNSRE*, vol. 13, no. 3, pp. 311–324, 2005.

[14] P.-H. Kuo and A. D. Deshpande, "Muscle-tendon units provide limited contributions to the passive stiffness of the index finger metacarpophalangeal joint," *Jou. of Biomech.*, vol. 45, no. 15, pp. 2531–2538, 2012.

[15] P. Agarwal and A. D. Deshpande, "Impedance and force-field control of the index finger module of a hand exoskeleton for rehabilitation," in *IEEE ICORR*, 2015, pp. 85–90.

[16] A. W. Dromerick, "Clinical features of spasticity and principles of treatment," in *Cli. Eval. Manag. of Spasti.*, 2002, pp. 13–26.

[17] S. A. Chillag and S. Greenberg, "An Unusual Cause of Trigger Finger," *New England Journal of Medicine*, vol. 365, no. 7, 2011.

[18] N. Hogan, H. I. Krebs, B. Rohrer, J. J. Palazzolo, L. Dipietro, S. E. Fasoli, J. Stein, R. Hughes, W. R. Frontera, D. Lynch, *et al.*, "Motions or muscles? Some behavioral factors underlying robotic assistance of motor recovery," *Jour. of rehab. res. dev.*, vol. 43, no. 5, p. 605, 2006.

[19] P. Agarwal, J. Fox, Y. Yun, M. K. OMalley, and A. D. Deshpande, "An index finger exoskeleton with series elastic actuation for rehabilitation: Design, control and performance characterization," *The International Journal of Robotics Research*, vol. 34, no. 14, pp. 1747–1772, 2015.

[20] P. Agarwal, Y. Yun, J. Fox, K. Madden, and A. D. Deshpande, "Design, control, and testing of a thumb exoskeleton with series elastic actuation," *IJRR*, vol. 36, no. 3, pp. 355–375, 2017.

[21] D. Zanotto, P. Stegall, and S. K. Agrawal, "Adaptive assist-as-needed controller to improve gait symmetry in robot-assisted gait training," in *IEEE ICRA*, 2014, pp. 724–729.

[22] X. Jin, X. Cui, and S. K. Agrawal, "Design of a cable-driven active leg exoskeleton (c-alex) and gait training experiments with human subjects," in *IEEE ICRA*, 2015, pp. 5578–5583.

[23] A. Pedrocchi, S. Ferrante, E. Ambrosini, M. Gandolla, C. Casellato, T. Schauer, C. Klauer, J. Pascual, C. Vidaurre, M. Gföhler, *et al.*, "MUNDUS project: MUltimodal Neuroprosthesis for daily Upper limb Support," *Journal of Neuroengg. and Rehab.*, vol. 10, p. 66, 2013.

[24] E. T. Wolbrecht, V. Chan, D. J. Reinkensmeyer, and J. E. Bobrow, "Optimizing compliant, model-based robotic assistance to promote neurorehabilitation," *IEEE TNSRE*, vol. 16, no. 3, pp. 286–297, 2008.

[25] A. U. Pehlivan, F. Sergi, and M. K. O'Malley, "A Subject-Adaptive Controller for Wrist Robotic Rehabilitation," *IEEE/ASME Transactions on Mechatronics*, vol. PP, no. 99, pp. 1–13, 2014.

[26] A. U. Pehlivan, D. P. Losey, and M. K. O'Malley, "Minimal assist-as-needed controller for upper limb robotic rehabilitation," *IEEE Transactions on Robotics*, vol. 32, no. 1, pp. 113–124, 2016.

[27] J. Klein, S. J. Spencer, and D. J. Reinkensmeyer, "Breaking it down is better: haptic decomp. of complex movements aids in robot-assisted motor learning," *IEEE TNSRE*, vol. 20, no. 3, pp. 268–275, 2012.

[28] P. Agarwal, B. R. Fernandez, and A. D. Deshpande, "Assist-as-needed controllers for index finger module of a hand exoskeleton for rehabilitation," in *ASME DSCC*, 2015, pp. DSCC2015–9790.

[29] P. Agarwal and A. D. Deshpande, "Series elastic actuators for small-scale robotic applications," *JMR*, vol. 9, no. 3, p. 031016, 2017.

[30] L. L. Cai, A. J. Fong, C. K. Otoshi, Y. Liang, J. W. Burdick, R. R. Roy, and V. R. Edgerton, "Implications of Assist-As-Needed Robotic Step Training after a Complete Spinal Cord Injury on Intrinsic Strategies of Motor Learning," *The Jour. of Neurosci.*, vol. 26, no. 41, Oct. 2006.

[31] N. Karnati, B. A. Kent, and E. D. Engeberg, "Bioinspired sinusoidal finger joint synergies for a dexterous robotic hand to screw and unscrew objects with different diameters," *IEEE/ASME Transactions on Mechatronics*, vol. 18, no. 2, pp. 612–623, 2013.

[32] A. Esteki and J. M. Mansour, "An experimentally based nonlinear viscoelastic model of joint passive moment," *Journal of Biomechanics*, vol. 29, no. 4, pp. 443–450, 1996.

[33] D. Wettschereck and T. Dietterich, "Improving the performance of radial basis function networks by learning center locations," in *NIPS*, vol. 4, 1991, pp. 1133–1140.

[34] B. Karlik and A. V. Olgac, "Performance analysis of various activation functions in generalized mlp architectures of neural networks," *Int. J. Artificial Intell. Expert Syst*, vol. 1, no. 4, pp. 111–122, 2011.

[35] J. Moody and C. J. Darken, "Fast learning in networks of locally-tuned processing units," *Neural comp.*, vol. 1, no. 2, pp. 281–294, 1989.

[36] K. Kuczynski, "The proximal interphalangeal joint anatomy and causes of stiffness in the fingers," *Journal of Bone & Joint Surgery, British Volume*, vol. 50, no. 3, pp. 656–663, 1968.

[37] B. H. Helal, "Extra-articular causes of PIP joint stiffness in rheumatoid arthritis," *The Hand*, vol. 7, no. 1, pp. 37–40, 1975.

[38] D. H. Harrison, "The stiff proximal interphalangeal joint," *The Hand*, vol. 9, no. 2, pp. 102–108, 1977.